32nd URSI GASS, Montreal, 19-26 August 2017

The USU-GAIM-FP Data Assimilation Model for Ionospheric Specifications and Forecasts

Ludger Scherliess*, Robert W. Schunk, Larry C. Gardner, J. Vincent Eccles, Lie Zhu, and Jan J. Sojka
Center for Atmospheric and Space Sciences, Utah State University, Logan, UT, USA

Abstract

Physics-based data assimilation models have been used in meteorology and oceanography for several decades and are now becoming prevalent for specifications and forecasts of the ionosphere. This increased use of ionospheric data assimilation models coincides with the increase in data suitable for assimilation. At USU we have developed several different data assimilation models, including the Global Assimilation on Ionospheric Measurements Gauss-Markov (GAIM-GM) and the Full Physics (GAIM-FP) models. Both models assimilate a variety of different data types, including ground-based GPS/TEC, occultation, bottomside electron density profiles from ionosondes, in-situ electron densities, and space-based UV radiance measurements and provide specifications and forecasts on a spatial grid that can be global, regional, or local. While GAIM-GM is a simpler model that uses a statistical process in the Kalman filter, GAIM-FP is based on a more sophisticated Ensemble Kalman filter technique together with a physics-based ionosphere-plasmasphere model (IPM). The primary GAIM-FP output is in the form of 3-dimensional electron density distributions from 90 km to near geosynchronous altitude but also provides auxiliary information about the global distributions of the self-consistent ionospheric drivers (neutral winds and densities, electric fields). The GAIM-FP model has recently been updated and extended to include the ionospheric D-region and to incorporate bubble information obtained from the SSUSI instruments. Furthermore, additional data types have been added to the list of possible observations that can be assimilated. This list includes slant TEC observations form satellite-to-satellite and satellite-to-ground radio beacons as well as radio occultation data and in situ plasma density observations from generic satellites.

1. Introduction

At Utah State University, two physics-based Kalman-filter data assimilation models for the Earth's ionosphere have been developed. These models are the Gauss-Markov Kalman Filter Model (GAIM-GM) and the Full Physics-Based Kalman Filter Model (GAIM-FP) [*Scherliess et al.,* 2006, 2009]. Both models are part of the Global Assimilation of Ionospheric Measurements (GAIM) project [*Schunk et al.,* 2004a,b, 2005a,b, 2011; *Scherliess et al.,* 2004, 2006, 2009, 2011; *Jee et al.,* 2007, 2008; *Sojka et al.,* 2007; *Thompson et al.,* 2006, 2009; *Zhu et al.,* 2006].

Some of the data that have previously been assimilated by these models include phase-leveled ground-based Global Positioning Satellite (GPS) slant total electron content (TEC); bottomside electron density profiles from ionosonde/digisonde in Standard Archiving Output (SAO) data files; radio occultation (RO) slant total electron content data from the Constellation Observing System for Meteorology, Ionosphere, and Climate (COSMIC) Precision Omni-directional Dipole (POD) antennas; topside ionospheric plasma electron density measurements from the Defense Meteorological Satellite Program (DMSP) in situ sensors; and DMSP Special Sensor Ultraviolet Spectrographic Imager (SSUSI) and Special Sensor Ultraviolet Limb Imager (SSULI) nighttime UV radiances. Data reduction utilities are used to reduce the raw data files and provide data in an appropriate form for the GAIM models to assimilate. The reduction utilities can be adapted for both historical and real-time executions of the GAIM models. In order to increase the use of latent data, both models accept in its real-time mode (nowcast) the data with a latency of 3 hours.

2. GAIM-FP

The GAIM-FP model is based on an ensemble Kalman filter approach [*Evensen* , 2003] and rigorously evolves the ionosphere and plasmasphere electron density field and its associated errors using a physics-based Ionosphere-Plasmasphere model (IPM) [*Scherliess et al.,* 2004; *Schunk et al.,* 2004a]. The IPM is based on a numerical solution of the ion and electron continuity and momentum equations and covers the low and mid-latitudes from 90 to 30,000 km altitude [*Schunk et al.*, 2003]. The equations are solved along magnetic field lines for individual flux tubes of plasma, and the 3-D nature of the model is obtained by following a large number of plasma flux tubes. The 3-D distribution is obtained by mapping the results on a geographic grid. The IPM model uses the International Geomagnetic Reference Field (IGRF) [*Finlay et al.,* 2010], which

properly accounts for the displacement between the geomagnetic and geographic equators and the bending of the magnetic field lines with latitude. In its current version, the model does not assimilate data in the regions poleward of ~ ±60° geomagnetic latitude due to the vastly different physical processes that govern the high-latitude ionosphere, e.g., convection electric fields, particle precipitation.

GAIM-FP provides specifications of the 3-dimensional electron and ion (NO^+, O_2^+, N^+, O^+, H^+, He^+) density distributions from 90 km to near-geosynchronous altitude (~30,000 km). In addition, the model can provide the global distribution of the ionospheric drivers (electric field, neutral wind and composition) that are consistent with the ionospheric observations. It is important to note that the estimation of the ionospheric drivers is an integral part of our ensemble Kalman filter and is achieved by using the internal physics-based model sensitivities to the various driving forces. In this procedure, the ionospheric data are used to adjust the plasma densities and its drivers so that a consistency between the observations (within their errors) and the physical model is achieved. As a result, the assimilation procedure produces the optimal model-data combination of the ionosphere-plasmasphere system together with the set of drivers (electric fields, neutral winds, and composition) consistent with the ionospheric observations [*Scherliess et al.,* 2009, 2011].

3. Assimilation of New Data Types

The GAIM-FP model has recently been modified to assimilate slant TEC observations from satellite-to-satellite and satellite-to-ground radio beacons as well as radio occultation data and in situ plasma density observations from generic satellites. This extension of the model enables GAIM-FP to assimilate, for example, slant TEC from the network of DORIS ground stations, radio occultation data from the fleet of COSMIC-2 satellites and in situ density observations from satellites in circular or eccentric orbits.

To date this new capability of the model has only been explored using synthetic (model generated) observations. For this a "truth" run was generated using the IPM model with modified input parameters. The obtained IPM model densities were then used to generate synthetic data that mimicked those from real observation systems (e.g., the COSMIC-2 satellite constellation). Finally, the synthetic data were assimilated in the updated GAIM-FP model. Figure 1 shows an example of the improvements to the model assimilating in situ electron density observations. For this a skill score was computed that measures the improvements of the model specifications with respect to a background model run (GAIM-FP with only assimilating ground-based TEC, ionosondes and COSMIC-1 radio occultation data). The range of the skill score is from –infinity to 1. With similar results having a value of zero in this range and a score greater that zero indicates improvement over the background run. The top panel of Figure 1 shows a skill score for various altitudes for electron density as listed in the key at the top right. The bottom panel shows the skill score for the standard ionospheric parameters TEC, NmF2, and hmF2. It can clearly be seen that the skill scores are near or above zero, suggesting that the in situ data did not degrade the background solution and in most instances had a positive impact on the solution.

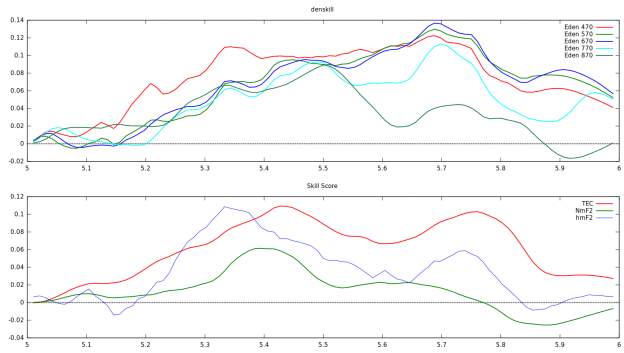

Figure 1. Skill scores for various altitudes (top) and ionospheric parameters (bottom) for GAIM-FP assimilating in situ electron density observations for January 5, 2013.

4. D-Region Extension

Recently, GAIM-FP has been extended to include a Data-Driven D-region model (DDDR) [*Eccles et al.,* 2005] that extends the lower boundary of the model down to 34 km altitude. Within the DDDR, the solar x-rays are modeled as hard x-rays (0.1 Å < l < 10 Å) and soft x-rays (10 Å < l, 100 Å). The GOES x-ray instruments observe hard x-rays in two integrated bands; 0.5-4 Å and 1-8 Å. These are overlapping bands of x-rays that impact the D region densities in the lower altitudes from 40 to 60 km. It is the soft x-rays that have significant impact on ionization in the 60 to 90 km altitudes. Within the DDDR, the flux and ratio of the GOES x-ray bands are used to populate hard and soft x-ray energy-flux bins. The absorption cross sections for the hard and soft x-rays are from *Banks and Kockarts* [1973] with updates from *Pavlov* [2013]. The x-ray ionization creates energetic secondary electrons or Compton photons that have sufficient energy for further ionization. It is assumed all secondary ionization occurs locally in the lower E region and D region with an ion-electron pair created for each 35 eV available in the energetic photon [*Banks and Kockarts*, 1973]. The DDDR also includes Lyman Alpha ionization of Nitric Oxide as an important source of D-Region ionization. The absorption cross-sections and ionization cross-sections for Lyman Alpha are from *Pavlov* [2013].

The DDDR nighttime ionization is created from geocorona resonant emissions, interplanetary gas scatter (He II, He I, Lyman Alpha) and starlight [*Strobel et al.,*

1980; *Titheridge*, 2001]. These nighttime ionization rates within the DDDR are dependent on F10.7 and (nighttime) solar angle.

Energetic electron precipitation from the auroral region is determined from the oval model of *Hardy et al.* [1985, 1987]. The calculation of ionization due to energetic electrons uses the characteristic energy and flux provided by the climatological Hardy oval model to create an electron energy distribution at the top of the ionosphere [*Robinson et al.*, 1986]. The topside electron energy fluxes are then used to calculate an ionization profile using primary fluxes and secondary electron production. Finally, average ionization profiles are used to model Solar Proton Events using the GOES energetic proton flux observations and cutoff rigidity formulae [Smart and Shea, 2005].

5. Bubble Incorporation

Although GAIM-FP does not include the physical processes that drive ionospheric plasma instabilities and bubbles, information about the location and extend of ionospheric bubbles has recently been incorporated into the model. The bubble information is obtained from the HiRes SSUSI 3-D ionosphere product and consists of the plasma-depletion centroid location (longitude, latitude, altitude) and the median depth of the plasma depletion.

The GAIM bubble incorporation is designed, first, to interpolate the electron density field from GAIM-FP to a sufficient resolution for resolving larger plasma bubble structures (>50 km), and, second, to produce a new output file containing a high-resolution specification of the electron densities with field-aligned density depletions based on the HiRes SSUSI observations. The HiRes SSUSI NetCDF files are currently used in the program. This Bubble Mapping program uses the depletion region characteristics within the HiRes SSUSI files to initiate the field-line plasma bubble definition which is imposed on the high-resolution interpolation of the GAIM-FP electron density specification.

For each time of GAIM output, the mapping program examines all depletions found within the SSUSI data files for the current and previous UT day. Only depletions that reside in the current nighttime regions are retained for the specification. These observed depletions are assumed to extend along magnetic field-lines. This assumption is well founded on observations and theory of the low-latitude ionosphere structure. Each plasma depletion (bubble) in the final electron density output is generated by, first, numerically tracing along the field line that pierces the observed centroid of the depletion. This properly extends the plasma depletion through the low-latitude F region beyond the SSUSI observation. Figure 2 shows an example of the GAIM electron densities at 1500 UT for day 078/2013. The top panel shows a longitude/altitude slice through the 3-dimensional electron density field as provided by GAIM at the geographic equator. The bottom panel shows the interpolated density field together with the superposed plasma depletions. These interpolated output files with superposed plasma bubbles can be useful for user applications that need higher resolution input with medium-scale plasma structures. For example, sensitive mathematical procedures, such as ray-tracing programs, benefit from the higher resolution and the communications breakups generated by irregularity structures in the background ionosphere.

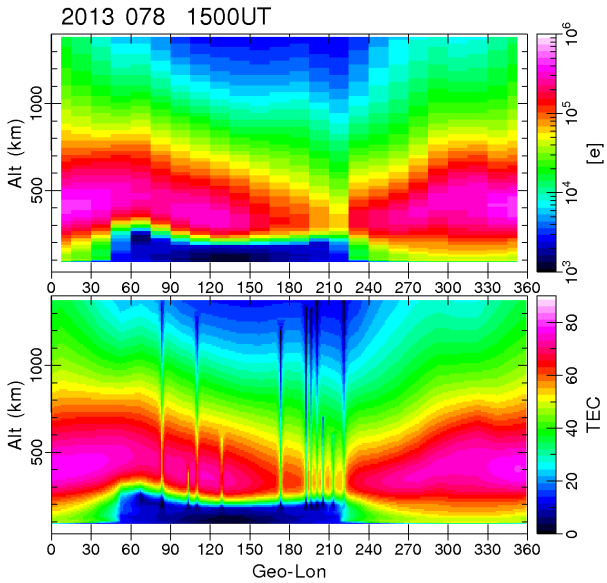

Figure 2. GAIM results in top panel. Interpolated & bubble results in bottom panel. Both are a longitude slice at the geographic equator.

6. Summary and Conclusion

The USU GAIM-FP model is based on a sophisticated Ensemble Kalman filter technique together with a physics-based ionosphere-plasmasphere model (IPM). The model assimilates measurements from various ionospheric observing systems and allow for data latencies of up to 3 hours. Recently, the model has been updated and extended to include ionospheric bubble information and a data-driven D-region model and can now assimilate slant TEC observations form satellite-to-satellite and satellite-to-ground radio beacons as well as radio occultation data and in situ plasma density observations from generic satellites.

7. References

Banks, P. M., and G. Kockarts (1973), Aeronomy, Academic, San Diego, Calif.

Eccles, J. V., R. D. Hunsucker, D. Rice, and J. J. Sojka (2005), Space weather effects on midlatitude HF propagation paths: observations and a data-driven D-region model, *Space Weather Journal, 3,* S01002, doi:10.1029/2004SW000094.

Evensen, G. (2003), The Ensemble Kalman Filter: Theoretical Formulation and Practical

Implementation, *Ocean Dynamics*, *53*, 343–367, DOI 10.1007/s10236-003-0036-9.

Finlay, C. C., et al. (2010), International geomagnetic reference field: The eleventh generation, Geophys. J. Int., 183, 1216–1230, doi:10.1111/j.1365-246X.2010.04804.x.

Hardy, D. A., M. S. Gussenhoven, and E. Holeman (1985), A statistical model of the auroral electron precipitation, J. Geophys. Res., 90 4229.

Hardy, D. A., M. S. Gussenhoven, R. Raistrick, and W. J. McNeil (1987), Statistical and functional representations of the pattern of auroral energy flux, number flux and conductivity, J. Geophys. Res., 92, 12,275-12,594.

Jee, G., A. G. Burns, W. Wang, S. C. Solomon, R. W. Schunk, L. Scherliess, D. C. Thompson, J. J. Sojka, and L. Zhu (2007), Duration of an ionospheric data assimilation initialization of a coupled thermosphere-ionosphere model, Space Weather, 5 (1), doi:10.1029/2006SW000250.

Jee, G., A. G. Burns, W. Wang, S. C. Solomon, R. W. Schunk, L. Scherliess, D. C. Thompson, J. J. Sojka, and L. Zhu (2008), Driving the TING model with GAIM electron densities: Ionospheric effects on the thermosphere, J. Geophys. Res., 113 (A3), doi:10.1029/2007JA012580.

Pavlov, A. V. (2013), Photochemistry of ions at D-region altitudes of the ionosphere: A review, Surv. Geophys., DOI 10.1007/s10712-013-9253-z.

Robinson, R. M., R. R. Vondrak, K. Miller, T. Dabbs, and D. Hardy (1987), On calculating ionospheric conductances from the flux and energy of precipitating electrons, J. Geophys. Res., 92, 2565-2569.

Scherliess, L., R. W. Schunk, J. J. Sojka, and D. Thompson (2004), Development of a physics-based reduced state Kalman filter for the ionosphere, Radio Sci., 39 (RS1S04), doi:10.1029/2002RS002797.

Scherliess, L., R. W. Schunk, J. J. Sojka, D. C. Thompson, and L. Zhu (2006), Utah State University Global Assimilation of Ionospheric Measurements Gauss-Markov Kalman filter model of the ionosphere: Model description and validation, J. Geophys. Res., 111 (A11315), doi:10.1029/2006JA011712.

Scherliess, L., D. C. Thompson, and R. W. Schunk (2009), Ionospheric dynamics and drivers obtained from a physics-based data assimilation model, Radio Sci., 44 (RS0A32), doi:10.1029/2008RS004068.

Scherliess, L., D. C. Thompson, and R. W. Schunk (2011), Data assimilation models: A new tool for ionospheric science and applications, in The Dynamic Magnetosphere, IAGA Special Sopron Book Series, vol. 3, edited by W. Liu and M. Fujimoto, pp. 329–339, Springer, Berlin.

Schunk, R. W., J. V. Eccles, J. J. Sojka, D. C. Thompson and L. Zhu (2003), Assimilation Ionosphere Model (AIM), *Final Report*, Space Environment Corporation.

Schunk, R. W., et al. (2004a), Global Assimilation of Ionospheric Measurements (GAIM), Radio Sci., 39 (RS1S02), doi:10.1029/2002RS002794.

Schunk, R. W., L. Scherliess, J. J. Sojka, and D. C. Thompson (2004b), USU global ionospheric data assimilation models, Proc. SPIE, 5548, 327–33 doi:10.1117/12.562448.

Schunk, R. W., L. Scherliess, J. J. Sojka, D. C. Thompson, and L. Zhu (2005a), An operational data assimilation model of the global ionosphere, Proc. Ionospheric Effects Symposium, edited by J. M. Goodman, 512-518 pp., JMG Assoc., Alexandria, Va.

Schunk, R. W., L. Scherliess, J. J. Sojka, D. C. Thompson, and L. Zhu (2005b), Ionospheric weather forecasting on the horizon, *Space Weather, 3*, S08007, doi:10.1029/2004SW000138.

Schunk, R. W., L. Scherliess, and D. C. Thompson (2011), Ionosphere data assimilation: Problems associated with missing physics, in Aeronomy of the Earth's Atmosphere and Ionosphere, IAGA Special Sopron Book Series, vol. 2, edited by D. P. M. Ali Abdu and A. Bhattacharyya, pp. 437–442, Springer, Berlin.

Smart, D.F., and M. A. Shea (2005), A review of geomagnetic cutoff rigidities for earth-orbiting spacecraft, Adv. Space res., 36, p2012-2020.

Sojka, J. J., D. C. Thompson, L. Scherliess, R. W. Schunk, and T. J. Harris (2007), Assessing models for ionospheric weather specifications over Australia during the 2004 Climate and Weather of the Sun-Earth-System (CAWSES) campaign, J. Geophys. Res., 112 (A9), doi:10.1029/2006JA012048.

Strobel, D. F., C. B. Opal, and R. R. Meier (1980), Photoionization rates in the nighttime E- and F-Region ionosphere, Planet. Space Sci., 28, 1027-1033.

Thompson, D. C., L. Scherliess, J. J. Sojka, and R. W. Schunk (2006), The Utah State University Gauss-Markov Kalman filter of the ionosphere: The effects of slant TEC and electron density profile data on model fidelity, J. Atmos. Sol. Terr. Phys., 68, 947–958.

Thompson, D. C., L. Scherliess, J. J. Sojka, and R. W. Schunk (2009), Plasmasphere and upper ionosphere contributions and corrections during the assimilation of GPS slant TEC, Radio Sci., 44 (1), doi:10.1029/2008RS004016.

Titheridge, J. E. (2001), Production of the low-latitude night E layer, J. Geophys. Res., 106, 12,781-12,786.

Zhu, L., R. W. Schunk, G. Jee, L. Scherliess, J. J. Sojka, and D. C. Thompson (2006), Validation study of the Ionosphere Forecast Model using the TOPEX total electron content measurements, Radio Sci., 41 (5), doi:10.1029/2005RS003336.